Electronic structure of InAs$(\bar{1}\,\bar{1}\,\bar{1})2\times2$ and InSb$(\bar{1}\,\bar{1}\,\bar{1})2\times2$ studied by angle-resolved photoelectron spectroscopy

C. B. M. Andersson and U. O. Karlsson
Materials Physics, Department of Physics, The Royal Institute of Technology, S-100 44 Stockholm, Sweden

M. C. Håkansson
Department of Synchrotron Radiation Research, Institute of Physics, Lund University, Sölvegatan 14, S-223 62 Lund, Sweden

L. Ö. Olsson, L. Ilver, P.-O. Nilsson, and J. Kanski
Department of Physics, Chalmers University of Technology, S-412 96 Göteborg, Sweden

P. E. S. Persson
SAAB AB, SAAB Military Aircraft, S-581 88 Linköping, Sweden
(Received 7 February 1996)

The electronic structure of molecular-beam-epitaxy-grown InAs$(\bar{1}\,\bar{1}\,\bar{1})2\times2$ and InSb$(\bar{1}\,\bar{1}\,\bar{1})2\times2$ surfaces is investigated by angle-resolved photoelectron spectroscopy. Valence-band spectra, and dispersions of five surface-related structures, are presented. The qualitative similarities of data from the two surfaces indicate that they are very similar, with respect to atomic and electronic structure. Comparisons with other (111) surfaces support the identification of the surface-related structures. [S0163-1829(96)00927-7]

INTRODUCTION

Polar In-based III-V semiconductor surfaces exhibit a large variety of reconstructions, depending on sample orientation and surface preparation.[1] The group-III terminated (111) surfaces show 2×2 reconstructions, consistent with a vacancy model.[1–6] The group-V terminated (1 1 1) side exhibits a number of different reconstructions. When prepared by repeated cycles of sputtering and annealing, the InAs(1 1 1) surface is unreconstructed,[6,7] while InSb(1 1 1) has a 3×3 surface periodicity.[8] Preparation by molecular-beam epitaxy (MBE) under group-V-rich conditions results in a 2×2 reconstruction for both InAs and InSb. Core-level spectra from these surfaces[9] are consistent with a surface model of group-V trimers, bonded to group-V atoms in the topmost complete double layer, as illustrated in Fig. 1. Also included in the figure is the geometry of the surface Brillouin zone (SBZ). The trimer geometry was originally proposed by Kaxiras *et al.*,[10–13] and confirmed experimentally in the case of InSb by Nakada and Osaka.[14] Several studies have been

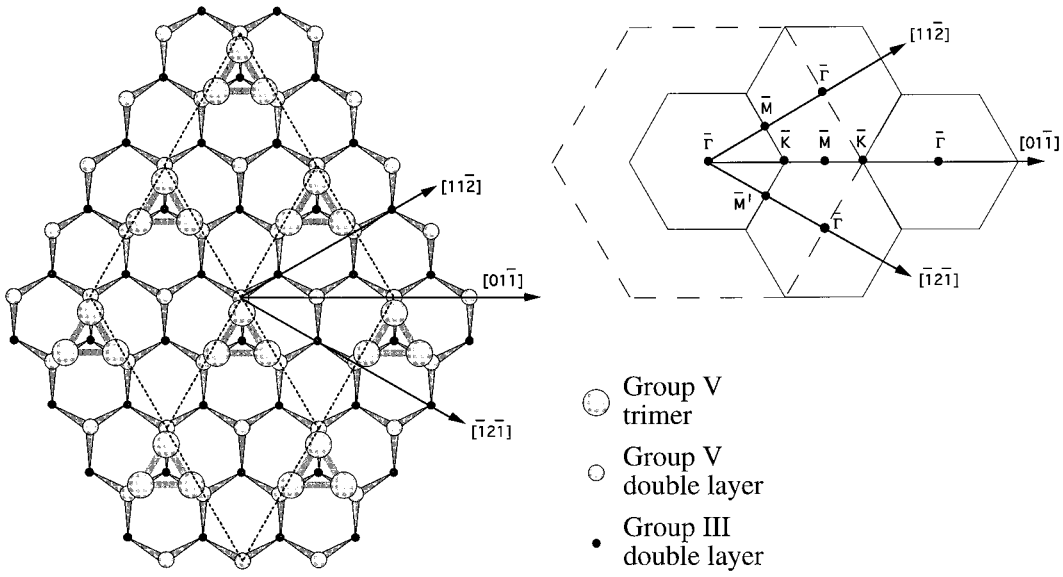

FIG. 1. Top view of the trimer model for the $(\bar{1}\,\bar{1}\,\bar{1})2\times2$ reconstruction. The 2×2 surface unit cell is indicated with dashed lines. Also shown is the SBZ. The 2×2 SBZ is indicated with solid lines, while the 1×1 SBZ is drawn as a dashed hexagon. $\bar{\Gamma}\,\bar{M}$ is defined as the backbond azimuth [112], and $\bar{\Gamma}\,\bar{M}'$ as the antibackbond azimuth [121] for the (1 1 1) surface. All points marked out refer to the 2×2 SBZ.

performed of the electronic structure of As-rich GaAs(1 1 1)2×2,[15–22] while to date the electronic structure of the corresponding InAs and InSb surfaces are not discussed in the literature. For the GaAs(1 1 1) surface, another 2×2 reconstruction with a lower As concentration in the surface layer has also been reported.[22–24] To investigate whether the 2×2 reconstruction is system specific or dictated by general features of the (1 1 1) surface, the valence-band electronic structure of the MBE-grown, group-V-rich, InAs(1 1 1)2×2 and InSb(1 1 1)2×2 surfaces is studied by means of angle-resolved photoelectron spectroscopy (ARPES). Five surface-related structures S_1-S_5 are identified, with qualitatively the same $E_i(k_\parallel)$ dispersions for the two surfaces. Comparisons are made with spectra of the group-V-rich GaAs(1 1 1)2×2 surface found in the literature,[15–18] as well as with other (111)-type surface reconstructions of InAs and InSb.[5–7]

EXPERIMENT

The angle resolved photoelectron spectra were recorded with a modified Vacuum Science Workshop Ltd. ARIES system, at the toroidal-grating monochromator beamline at the MAX synchrotron radiation facility in Lund, Sweden.[25] Connected to the photoemission system is an MBE system, equipped with six effusion cells and reflection high-energy electron diffraction (RHEED). The spectra, excited in *p* polarization with a photon incidence angle of 45°, were detected in the plane of incidence. The initial-state energy scale is referred to the Fermi level (E_F), determined by measurements on a Ta foil in electrical contact with the sample. The InAs(1 1 1) substrate was *n* type ($n=8.7\times10^{16}$ cm^{-3}), and the InSb(1 1 1) substrate was *p* type ($p=2\times10^{13}$ cm^{-3}). Both wafers were supplied by MCP Wafer Technology, Ltd., England. The initial surfaces were prepared *in situ* by repeated cycles of Ar-ion bombardment and annealing (IBA). The quality of the surfaces was monitored by low-energy electron diffraction (LEED) and ARPES of the valence band. After a few IBA cycles, the substrates showed sharp 1×1 (InAs) and 3×3 (InSb) LEED patterns. These substrates were transferred under ultrahigh vacuum to the MBE chamber for homoepitaxial growth under group-V-rich conditions. The growth was monitored by RHEED. Subsequent ARPES and LEED studies of the MBE-grown surfaces showed sharp core-level[9] and valence-band structures as well as very sharp 2×2 LEED patterns with low background. The original 1×1 and 3×3 surfaces reappeared at annealing temperatures above approximately 350 and 300 °C, respectively.

RESULTS

Spectra were recorded from the $(\bar{1}\,\bar{1}\,1)2\times2$ surfaces of InAs and InSb along the three azimuths $\bar{\Gamma}\,\bar{M}$, $\bar{\Gamma}\,\bar{M}'$, and $\bar{\Gamma}\,\bar{K}\,\bar{M}$ of the SBZ (see Fig. 1). The energy positions of spectral features originating from direct bulk interband transitions were calculated for the photon energies used in the experiment, with the final states approximated by free-electron parabolas with inner potentials 8 eV for InAs and 7 eV for InSb. The initial bands were obtained from a linear combination of atomic orbitals calculation.[26] This enables identification of bulk-related structures in the spectra, and is also used to distinguish between the two inequivalent $\bar{\Gamma}\,\bar{M}$ and $\bar{\Gamma}\,\bar{M}'$ azimuths. The theoretical bulk bands are also projected onto the SBZ to determine energy regions in *k* space, where no bulk-related initial states are present. For InAs, this projection is provided by another calculation, based on a combination of the linear augmented plane-wave method[27] and the relativistic augmented plane-wave method.[28] It was performed within the density-functional theory, using the Hedin-Lundquist local-density approximation for the exchange and correlation potential.[29]

In the case of InAs, the position of the valence-band maximum (VBM) relative to E_F is determined in three ways. From In 4*d* core-level spectra[9] a separation between the In $4d_{5/2}$ component and the Fermi level of 17.35±0.05 eV is obtained. With the literature value of the separation between the VBM and the In $4d_{5/2}$ bulk component of 16.91 eV,[30] a Fermi-level position of 0.44 eV above the VBM is obtained. The fundamental band gap of InAs is 0.36 eV; thus the Fermi level is located above the conduction-band minimum (CBM), and the conduction-band states below E_F are filled. Due to band bending at the surface, these electrons are confined to the surface region, and a quasi-two-dimensional electron gas is formed.[31] The confinement perpendicular to the surface leads to quantization. In normal-emission spectra, a structure is observed at E_F.[31] The lower edge of this structure corresponds to the lowest filled conduction-band state, which is situated at the CBM, or slightly above. Thus the width of this structure, 0.190±0.005 eV, is an estimate of the energy difference between E_F and the CBM, and a value for $(E_F-E_{\mathrm{VBM}})=0.55\pm0.05$ eV is obtained. Assuming that the onset of the next structure in the normal-emission spectra corresponds to the VBM, one obtains $(E_F-E_{\mathrm{VBM}})=0.55\pm0.10$ eV, in excellent agreement with the previous value. Accepting this value, a separation between the VBM and the In $4d_{5/2}$ bulk component of 16.80±0.10 eV is derived. This is consistent with data found in the literature.[30] From In 4*d* core-level spectra of InSb,[9] a separation between the In $4d_{5/2}$ component and the Fermi level of 17.39±0.05 eV is obtained. With a literature value of the separation between the VBM and the In $4d_{5/2}$ component of 17.20 eV,[32] a Fermi-level position of 0.19±0.10 eV above the VBM is obtained. The fundamental band gap of InSb is 0.18 eV, which indicates that the Fermi level is located at or slightly above the CBM. From normal-emission spectra it is estimated that $(E_F-E_{\mathrm{VBM}})=0.25\pm0.10$ eV. The values 0.55 (InAs) and 0.25 eV (InSb) are used in Figs. 3 and 4 for (E_F-E_{VBM}).

A set of spectra excited with a photon energy of 24 eV, recorded along the $\bar{\Gamma}\,\bar{K}\,\bar{M}$ azimuth of the InAs(1 1 1)2×2 surface, is presented in Fig. 2(a). A corresponding set for the InSb(1 1 1)2×2 surface, excited with 20 eV photons, is presented in Fig. 2(b). Similar structures are identified for both surfaces, and the candidates for surface-related structures, S_1-S_5, are indicated in the figures. Identification of the surface-related structures is based on the following criteria: they should disperse with the 2×2 symmetry of the SBZ, and have no dispersion along the surface normal. In addition, we also used the fact that in contrast to bulk states the $E_i(k_\parallel)$ dispersion of surface-related structures should be the same along the $\bar{\Gamma}\,\bar{M}$ and $\bar{\Gamma}\,\bar{M}'$ azimuths. The projected bulk bands and the calculated direct bulk interband transitions are

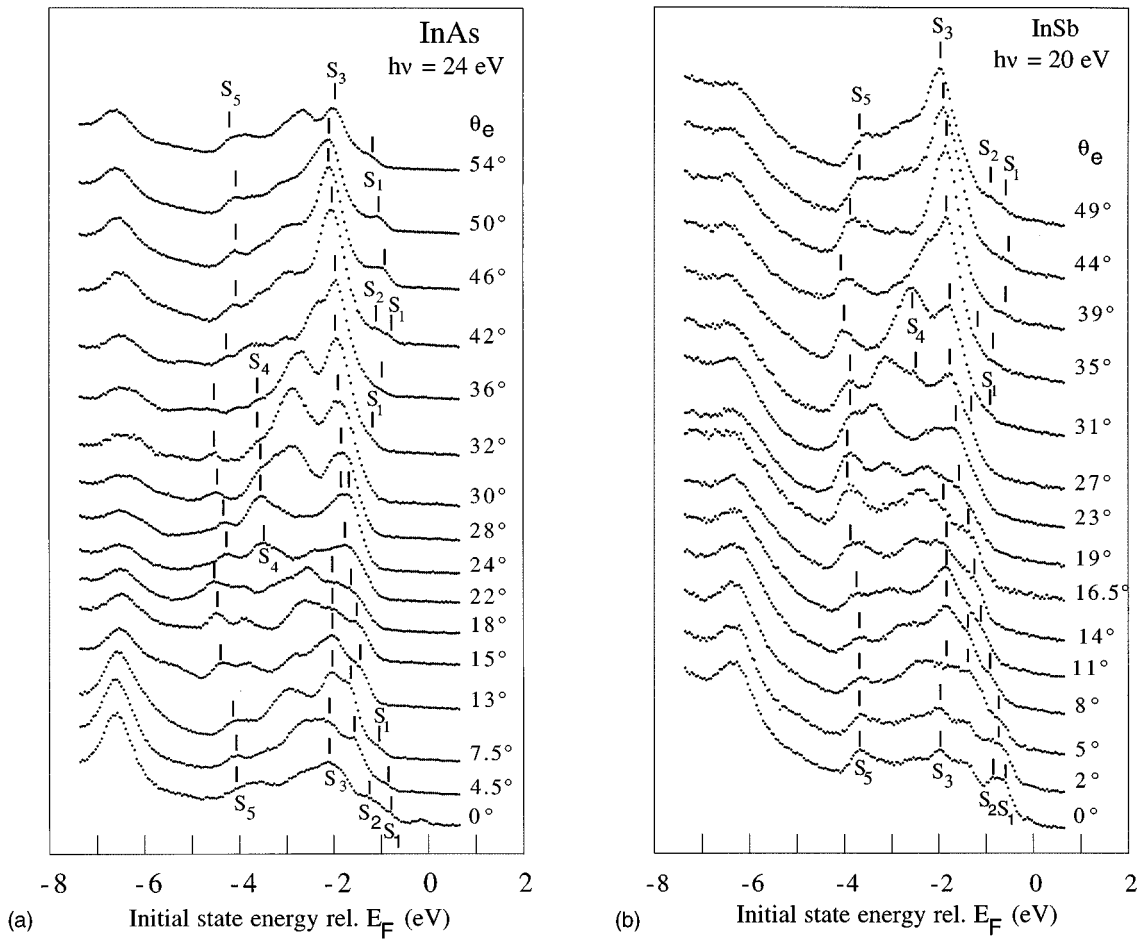

FIG. 2. (a) Photoelectron spectra as function of the emission angle recorded along the $\bar{\Gamma}\,\bar{K}\,\bar{M}$ azimuth with 24 eV photon energy for InAs(1 1 1)2×2. (b) Photoelectron spectra as function of emission angle recorded along the $\Gamma\ K\ M$ azimuth with 20 eV photon energy for InSb(1 1 1)2×2.

also used in the identification procedure.

The positions of S_1, S_2, S_3, and S_5 are marked in the normal-emission spectra. S_3 and S_5 are indicated in all of the spectra recorded at higher emission angles, while the other structures are weaker and distinguished only in some spectra. In most spectra, S_5 appears as a small distinct peak while S_3 is one of the dominating structures. S_3 overlaps with primary cone emission from the bulk at $\theta_e=0°$. When θ_e is increased, the bulk-related emission disperses downwards while S_3 disperses upwards. In spectra close to $M_{2\times2}$, $\theta_e=22°$ (InAs) and 19°–23° (InSb), the structures marked out correspond mainly to S_3. The long slope at higher initial-state energies corresponds to S_1, S_2, and the bulk valence-band edge, which all overlap. The bulk valence-band edge is known to give rise to features in spectra from other (111) surfaces.[5,8] S_1 is not indicated as a separate structure for 13°–30° (InAs) and 14°–27° (InSb) emission angles. At the first $K_{2\times2}$ point, 13° (InAs) and 14° (InSb), S_1 and S_2 overlap. For higher angles, S_2 is marked out in InAs spectra as a separate structure at 15°, 18°, 24°, and 42°. For InSb, the indicated structure corresponds to S_1 and S_2, that overlap for 16.5° and 27° emission angles. The structure S_4 is only identified in a limited part of the SBZ, indicated for 22°–32° in the InAs spectra series, and for 31°–35° in the InSb series, when it disperses through the region of the small open lens of the bulk band structure around $K_{1\times1}$.

To demonstrate the uniqueness and surface nature of the structures S_2–S_5, as well as the large differences in the electronic structure between different reconstructions on (111)-type surfaces, photoemission spectra recorded close to symmetry points of the SBZ are presented in Fig. 3. For InAs(1 1 1)1×1 the structure S, located close to the projected valence-band edge, is identified as the filled As dangling-bond state.[7] Structure D, which is weaker and interpreted as emission from a region of high density of bulk states close to the projected valence-band edge, is also marked in spectra from other (111) surfaces. Spectra recorded at the $K_{1\times1}$ point are compared in Fig. 3(a). Due to the partial overlap of the structures S_1 and S_2, their individual peak positions cannot be determined. The positions of S_1 and S_2 fall somewhere between the onset of the photoemitted structures and the structure denoted $S_{1\text{-}2}$. It is clearly seen that $S_{1\text{-}2}$, S_3, and S_4 are observed for two different photon energies in the InAs(1 1 1)2×2 and InSb(1 1 1)2×2 spectra, but are missing on InAs(1 1 1)1×1, InAs(111)2×2, and InSb(111)2×2. The presence and uniqueness of S_5 is most clearly displayed at the $\bar{M}_{1\times1}$ and $\bar{M}'_{1\times1}$ points, which correspond to the second $\Gamma_{2\times2}$ points along the $\Gamma\ M$ and $\Gamma\ M'$ azimuths [Figs. 3(b) and 3(c)]. The sharp peak corresponding to S_5 is absent for all the other surface reconstructions. S_3, which is clearly seen in all (1 1 1)2×2 spectra

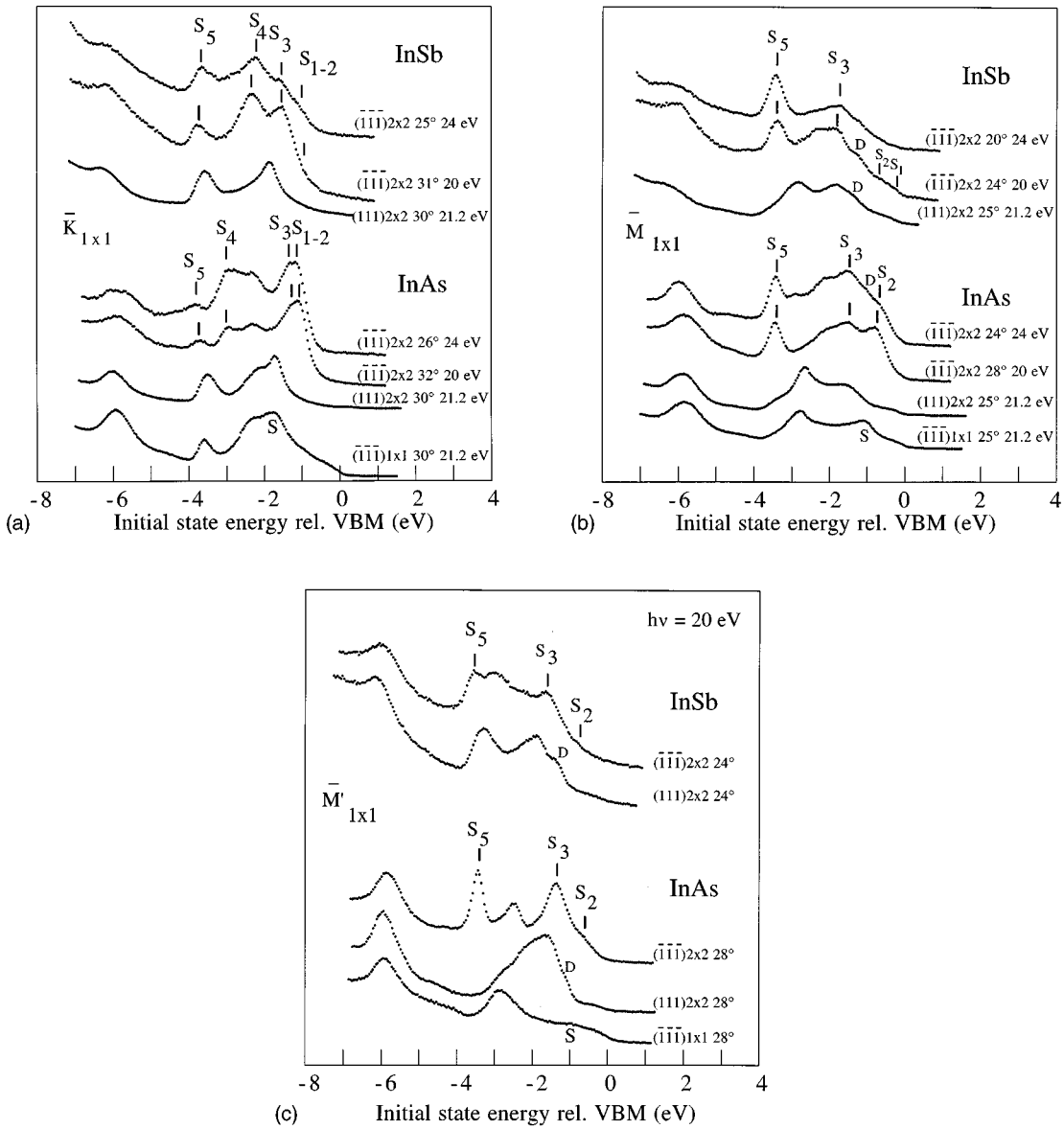

FIG. 3. (a) Comparison with spectra, recorded for other surface reconstructions (Refs. 5–7), close to $\overline{K}_{1\times1}$, corresponding to the second $\overline{K}_{2\times2}$. The spectra recorded for the $(1\,1\,\bar{1})2\times2$ surfaces are excited with synchrotron radiation, while the spectra from the other surfaces are excited with a He lamp. (b) Comparison with spectra, recorded for other surface reconstructions, (Refs. 5–7), close to $\overline{M}_{1\times1}$, corresponding to the second $\overline{\Gamma}_{2\times2}$. The spectra recorded for the $(1\,1\,\bar{1})2\times2$ surfaces are excited with synchrotron radiation, while the spectra from the other surfaces are excited with a He lamp. (c) Comparison with spectra, recorded for other surface reconstructions, (Refs. 5–7), close to $\overline{M}'_{1\times1}$, corresponding to the second $\overline{\Gamma}_{2\times2}$. All spectra are excited with synchrotron radiation with $h\nu=20$ eV.

at $\overline{\Gamma}_{2\times2}$, is absent in the InAs$(\bar{1}\,\bar{1}\,\bar{1})1\times1$ spectra. Close to this binding energy, a structure identified as surface induced[6] is present in spectra from InAs(111)2×2 and InSb(111)2×2. For InAs$(1\,1\,\bar{1})2\times2$, S_2 shows up as a unique and pronounced structure [Fig. 3(b)].

The $E_i(k_\parallel)$ dispersions for structures S_1-S_5 along the $\overline{\Gamma}\,\overline{M}$, $\overline{\Gamma}\,\overline{M}'$, and $\overline{\Gamma}\,\overline{K}\,\overline{M}$ azimuths of the SBZ are presented for InAs$(1\,1\,\bar{1})2\times2$ in Fig. 4(a), and for InSb$(1\,1\,\bar{1})2\times2$ in Fig. 4(b). The magnitude of $k_\parallel$ is given by $k_\parallel[\text{Å}^{-1}]=0.512\sin(\theta_e)\sqrt{E_{\text{kin}}}[\text{eV}]$, where E_{kin} is the kinetic energy of the photoelectron. The theoretically calculated bulk band structure, projected onto the unreconstructed SBZ, is indicated by the shaded areas. Data points in Fig. 4 have been connected with smooth lines, with the periodicity of the 2×2 SBZ, to indicate the likely dispersions of surface bands S_1-S_3 and S_5. Initial-state energies at the symmetry points of the 2×2 SBZ are given in Table I.

All structures overlap with the projected bulk valence bands for $k_\parallel=0$. When $k_\parallel$ is increased, S_1, S_2, and S_5 disperse downwards and S_3 disperses upwards, with S_1 closely following the projected valence-band edge. At the second $\overline{\Gamma}_{2\times2}$, S_1 and S_2 are located above the projected valence-band edge while S_5 is located in the big open lens of the projected bulk band structure. Emission from the high density-of-states region located close to the projected valence-band edge overlaps partly with S_1-S_3 and is also included in Fig. 4. The dispersions of the weak structures S_1 and S_2 are influenced by this overlap and are difficult to

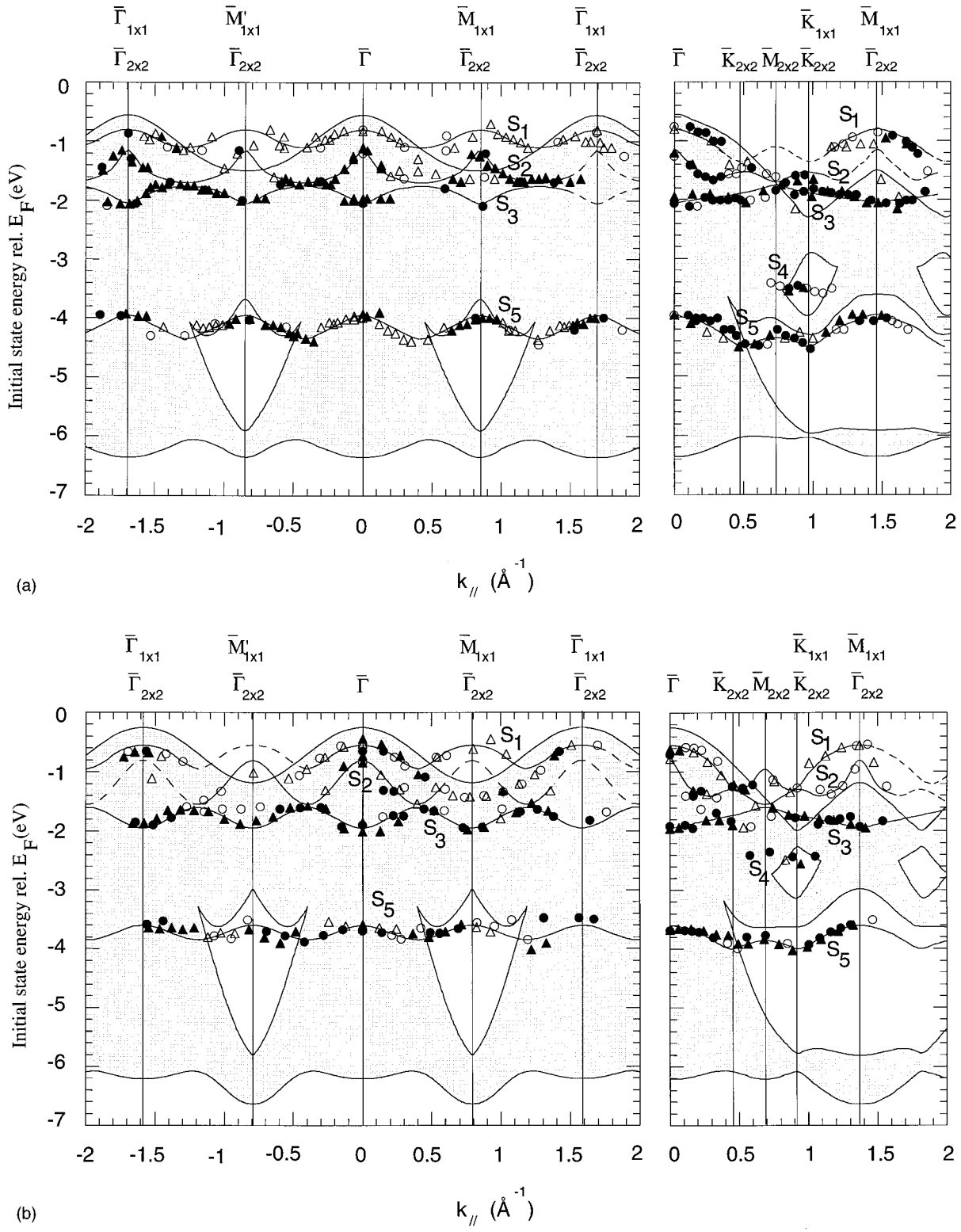

FIG. 4. (a) $E_i(k_\parallel)$ dispersions for structures S_1–S_5 along the $\bar{\Gamma}\,\bar{M}$, $\bar{\Gamma}\,\bar{M}'$, and $\bar{\Gamma}\,\bar{K}\,\bar{M}$ azimuths for InAs(1 1 1)2×2. The $\bar{\Gamma}\,\bar{M}$ azimuth is displayed as positive $k_\parallel$ values, and $\bar{\Gamma}\,\bar{M}'$ as negative. The theoretically calculated bulk band structure projected onto the SBZ is indicated by the shaded areas. To indicate the structures we have used circles for the photon energy 20 eV, and triangles for 24 eV. Filled symbols are used for relatively stronger or sharper structures. For the structures S_1–S_3 and S_5, we have drawn smooth lines to make it easier for the eye to follow the dispersions. (b) Same as in (a), but for InSb(1 1 1)2×2.

quantify. Due to the lack of reliable datapoints in the region of $K_{2\times2}$-$M_{2\times2}$-$K_{2\times2}$ for S_1 on InAs, we have indicated the ''probable'' band with a dashed line. The initial-state energy of a surface-related structure should be the same at $M_{2\times2}$ along all azimuths, and therefore the dispersion line is drawn upwards from $K_{2\times2}$ to $M_{2\times2}$. Dashed lines are also used in other parts of the $k_\parallel$ plot, where there are few data points.

The second $K_{2\times2}$ point coincides with $K_{1\times1}$. At this point

TABLE I. (a) Initial-state energies, relative to the VBM (eV), of the surface-related structures found for InAs at the symmetry points of the 2×2 SBZ. (b) Initial-state energies, relative to the VBM (eV), of the surface-related structures found for InSb at the symmetry points of the 2×2 SBZ.

(a)

	S_1	S_2	S_3	S_4	S_5
$\bar{\Gamma}$	−0.20	−0.55	−1.45		−3.35
$\bar{K}$:	−0.75	−0.95	−1.60	−2.90	−3.90
$\bar{M}$:	−0.50	−1.10	−1.15		−3.75
Bandwidth:	0.55	0.55	0.30		0.55

(b)

	S_1	S_2	S_3	S_4	S_5
$\bar{\Gamma}$:	−0.30	−0.55	−1.70		−3.35
$\bar{K}$:	−1.00	−1.10	−1.48	−2.30	−3.75
$\bar{M}$:	−0.70	−1.30	−1.35		−3.60
Bandwidth:	0.70	0.75	0.35		0.40

the projected bulk bands are limited to very narrow energy regions, leaving large energy regions free from contribution by direct bulk interband transitions. In this range, the surface-related structures are easily distinguished. None of the structures S_1-S_5 overlap with the projected bulk bands at $K_{1\times1}$. The identification of S_4 is done only along the Γ K M azimuth, where it disperses through the small open lens around the second $K_{2\times2}$.

DISCUSSION

Five candidates for surface-related structures have been indicated. They all display dispersion through the open lenses of the projected 1×1 bulk band structure or through the region above the projected valence-band edge. Although bulk-related structures may enter these parts of the SBZ through surface umklapp processes, such processes are generally weak.[33] Therefore these observations provide additional support for our assignment of structures S_1-S_5 as surface states.

It is clearly seen at $\bar{K}_{1\times1}$ [see Fig. 3(a)] that $S_{1\text{-}2}$, S_3, and S_4, in the InAs(1 1 1)2×2 and InSb(1 1 1)2×2 spectra are missing on InAs(111)2×2, InSb(111)2×2, and InAs(1 1 1)1×1. For S_5 the same is true at $\Gamma_{2\times2}$ [see Figs. 3(b) and 3(c)], S_5 also clearly demonstrates the 2×2 periodicity of the surface. We conclude that these structures are surface related and unique for the (1 1 1)2×2 reconstruction, and that the same structures S_1-S_5 are clearly identified for both InAs and InSb.

A surface geometry consisting of group-V trimers bonded to group-V atoms in the topmost complete double layer was shown by Nakada and Osaka[14] to stabilize the InSb(1 1 1)2×2 surface. Core-level spectra from the InAs(1 1 1)2×2 and InSb(1 1 1)2×2 surfaces[9] are found to be consistent with this surface model. Assuming that this model is valid, we next consider the various electron states. At the (1 1 1)2×2 surface, three-fourths of a monolayer of group-V atoms bind to the group-V atoms of the complete outermost double layer, thus reducing the number of original group-V dangling bonds. One group-V ''rest atom'' per 2×2 unit cell with one dangling bond remains (see Fig. 1). The group-V overlayer consists of trimers, and bonds are expected between the group-V atoms of the trimers within the surface plane, directed along the [110] direction, as well as a lone-pair orbital on each trimer atom. There also have to be backbonds between the trimer atoms and the atoms in the last complete group-V layer. Thus the following bonds are expected immediately at the surface (per 2×2 unit cell): (1) one filled dangling bond on the group-V rest atom, (2) three filled lone-pair orbitals on the group-V trimer, (3) three trimer bonds between atoms within the group-V trimer, and (4) three backbonds between atoms in the group-V trimer and group-V atoms in the double layer below.

These ten bonds accommodate 20 electrons. The number of available surface electrons in the valence band is 20 per 2×2 unit cell, 5×3 from the group-V atoms in the trimer, and 5/4 from each of the four group-V atoms in the double layer. From electron-counting principles, the defect-free surface should therefore be semiconducting. All these bonds are unique for the reconstruction, and give rise to surface states. Therefore surface-related structures are expected to influence the spectra strongly, and great differences in spectra from different reconstructions do indeed appear, as shown in Fig. 3.

To identify fully the origin of the individual structures based on the spectra presented here cannot be done, without a surface band-structure calculation based on the trimer model. It is possible, however, to make a tentative assignment based on the following observations. For other surfaces it is found that the dangling bonds and lone-pair orbitals are the most loosely bound and thus appear in the upper part of the valence band, while the other bonds are found further down.[1,7,34] Assuming that this tendency extends to the present cases, we attribute S_1-S_3, which appear within 1.8 eV of the VBM, to filled rest-atom dangling bonds and filled trimer lone-pair orbitals. The filled As dangling-bond state on the InAs(1 1 1)1×1 surface closely follows the dispersion of the upper edge of the projected bulk bands, and is the dominating feature in spectra.[7] In Fig. 3(b) this state is seen at −1 eV, yet it is missing on the other surfaces and thus uniquely belongs to the unreconstructed surface. On the 2×2 surfaces, S_1 closely follows the projected valence-band edge from the $\bar{\Gamma}$ point down to the first $K_{2\times2}$, $M_{2\times2}$, and $M'_{2\times2}$ along the three respective azimuths. In accordance with the 2×2 periodicity, S_1 turns upwards, crosses the valence-band edge, and enters the region above the projected bulk bands. The As dangling bond on the InAs(1 1 1)1×1 surface is strong at $\Gamma_{1\times1}$ and somewhat weaker at $M_{1\times1}$, the same is true for S_1 at $\Gamma_{2\times2}$ and $M_{2\times2}$. The band shape of S_1 and the As dangling-bond state dispersion on the 1×1 surface are similar, as well as their binding energies at Γ. Therefore we attribute S_1 to filled group-V rest-atom dangling-bond orbitals. S_4 and S_5 appear between −2.3 and −4 eV, which suggests that they reflect bonds between atoms in the surface or subsurface layer. The structures S_2-S_4 and S_5 are present on the (1 1 1)2×2 surfaces and absent on the InAs(1 1 1)1×1 and (111)2×2 surfaces at $K_{2\times2}$ and $\Gamma_{2\times2}$. Thus they uniquely belong to the trimer-induced 2×2 reconstruction. S_2 and S_3 are attributed to the lone-pair orbitals on the

group-V trimers, while S_4 and S_5 are attributed to bonds between group-V atoms within the trimer, or between trimer atoms and the double layer.

Valence-band spectra recorded for the GaAs$(\bar{1}\,\bar{1}\,\bar{1})2\times2$ surface in normal emission and at the symmetry points $\bar{M}_{1\times1}$, $\bar{M}'_{1\times1}$, and $\bar{K}_{1\times1}$ of the SBZ have been published by Bringans and Bachrach.[16,17] The corresponding spectra of InAs$(\bar{1}\,\bar{1}\,\bar{1})2\times2$ recorded at $\bar{M}_{1\times1}$ and $\bar{M}'_{1\times1}$, Figs. 3(b) and 3(c), are almost identical to the spectra of GaAs$(\bar{1}\,\bar{1}\,\bar{1})2\times2$. The resemblance to the corresponding spectra in normal emission and at $\bar{K}_{1\times1}$, Figs. 2(a) and 3(a), is also good, and it may be concluded that the same structure model should be applicable to the $(\bar{1}\,\bar{1}\,\bar{1})2\times2$ surfaces of all three materials. Bringans *et al.*[15] presented the $E_i(k_\parallel)$ dispersion of four surface-related structures along the lines $\bar{\Gamma}$-$\bar{K}$-$\bar{M}$ and $\bar{\Gamma}$-$\bar{M}$ of the SBZ. Comparing these with the $E_i(k_\parallel)$ dispersions of InAs$(\bar{1}\,\bar{1}\,\bar{1})2\times2$ and InSb$(\bar{1}\,\bar{1}\,\bar{1})2\times2$ presented in Fig. 4, we find that qualitatively the structures S_1-S_3 and S_5 correspond to the four structures found by Bringans *et al.* The polarization dependence, established by Bringans and Bachrach,[16] of the structures corresponding to S_1 and S_5 suggests that S_1 is derived from p_z states, and S_5 from orbitals not aligned with the surface normal.[16] Bringans *et al.*[15] attributed the structures corresponding to S_1, S_3, and S_5 to the rest-atom lone pair, the trimer lone pair, and As-As backbonds, respectively, in agreement with our discussion above.

Jacobi, Muschwitz, and Ranke[18] presented valence-band spectra of the As-rich GaAs$(\bar{1}\,\bar{1}\,\bar{1})2\times2$ surface recorded along the $\bar{\Gamma}\,\bar{M}'$ azimuth. A comparison with our structure plots in Fig. 4 shows that S_1, S_3, and S_5 are in agreement with the data on GaAs, while S_2 and S_4 are absent. The structure corresponding to S_3 was found to be reduced in *s* polarization, which suggests that S_3 is derived from p_z states.

In a normal-emission study by Cai *et al.*,[22] on two stoichiometrically different GaAs$(\bar{1}\,\bar{1}\,\bar{1})2\times2$ surfaces, structures in spectra corresponding to the two lowest surface bands identified in Refs. 16 and 17 were attributed to surface umklapp from bulk states. These structures appear in the same energy region as our structures S_3 and S_5. In our study, the identification of S_3 and S_5 as surface-related structures is also supported by the comparison with off-normal spectra from other reconstructions (see Fig. 3).

SUMMARY

From ARPES spectra we have identified five surface-related bands with similar dispersion for InAs$(\bar{1}\,\bar{1}\,\bar{1})2\times2$ and InSb$(\bar{1}\,\bar{1}\,\bar{1})2\times2$. This implies that the same structure model should be applicable to both surfaces. In the absence of a surface band-structure calculation, the origins of the surface-related structures are tentatively proposed. We attribute S_1 to filled rest-atom dangling bonds, S_2 and S_3 to filled lone-pair orbitals on the trimer atoms, and S_4 and S_5 to bonds between group-V atoms. S_3 and S_5 appear as dominating structures in spectra. Differences in the electronic structure of different reconstructions on (111)-type surfaces are demonstrated and support the identification of the surface-related structures. S_2-S_5 are absent on the InAs$(\bar{1}\,\bar{1}\,\bar{1})1\times1$ and $(111)2\times2$ surfaces, thus they uniquely belong to the trimer induced 2×2 reconstruction. The structures S_1-S_3 and S_5 identified for InAs$(\bar{1}\,\bar{1}\,\bar{1})2\times2$ and InSb$(\bar{1}\,\bar{1}\,\bar{1})2\times2$ are very similar to surface-related structures on GaAs$(\bar{1}\,\bar{1}\,\bar{1})2\times2$ reported by Bringans *et al.*[15] Therefore, the same structural model is probably applicable to all three surfaces.

ACKNOWLEDGMENTS

We would like to thank the staff at MAX-LAB for their technical assistance, and the Swedish Natural Science Research Council for their financial support.

[1] G. V. Hansson and R. I. G. Uhrberg, Surf. Sci. Rep. **9**, 197 (1988).
[2] C. B. Duke, J. Vac. Sci. Technol. B **11**, 1336 (1993).
[3] A. Khan, Surf. Sci. **299/300**, 469 (1994).
[4] J. M. C. Thornton, P. Unsworth, M. D. Jackson, P. Weightman, and D. A. Woolf, Surf. Sci. **316**, 231 (1994).
[5] L. Ö. Olsson, L. Ilver, J. Kanski, P. O. Nilsson, C. B. M. Andersson, U. O. Karlsson, and M. C. Håkansson, Phys. Rev. B **53**, 4734 (1996).
[6] C. B. M. Andersson, L. Ö. Olsson, M. C. Håkansson, L. Ilver, U. O. Karlsson, and J. Kanski, J. Phys. (France) IV **4**, C9-209 (1994).
[7] C. B. M. Andersson, U. O. Karlsson, M. C. Håkansson, L. Ö. Olsson, L. Ilver, J. Kanski, P.-O. Nilsson, and P. E. S. Persson, Surf. Sci. **307–309**, 885 (1994).
[8] L. Ö. Olsson, J. Kanski, L. Ilver, C. B. M. Andersson, M. Björkqvist, M. Göthelid, U. O. Karlsson, and M. C. Håkansson, Phys. Rev. B **50**, 18 172 (1994).
[9] C. B. M. Andersson, U. O. Karlsson, M. C. Håkansson, L. Ö. Olsson, L. Ilver, J. Kanski, and P.-O. Nilsson, Surf. Sci. **347**, 199 (1996)
[10] E. Kaxiras, Y. Bar-Yam, J. D. Joannopoulos, and K. C. Pandey, Phys. Rev. Lett. **57**, 106 (1986).
[11] E. Kaxiras, Y. Bar-Yam, J. D. Joannopoulos, and K. C. Pandey, Phys. Rev. (B) **35**, 9636 (1987).
[12] E. Kaxiras, Y. Bar-Yam, J. D. Joannopoulos, and K. C. Pandey, Phys. Rev. B **35**, 9625 (1987).
[13] E. Kaxiras, K. C. Pandey, Y. Bar-Yam, and J. D. Joannopoulos, Phys. Rev. Lett. **56**, 2819 (1986).
[14] T. Nakada and T. Osaka, Phys. Rev. Lett. **67**, 2834 (1991).
[15] R. D. Bringans, D. K. Biegelsen, L.-E. Swartz, and J. E. Northrup, *The Structure of Surfaces III*, edited by S. Y. Tong, M. A. Van Hove, K. Takayanagi, and X. D. Xie, Springer Series in Surface Science Vol. 24 (Springer, New York, 1991), p. 555
[16] R. D. Bringans and R. Z. Bachrach, Phys. Rev. Lett. **53**, 1954 (1984).
[17] R. D. Bringans and R. Z. Bachrach, in *Proceedings of the 17th International Conference on the Physics of Semiconductors*, edited by J. D. Chadi and W. A. Harrison (Springer-Verlag, New York, 1985), p. 67.
[18] K. Jacobi, C. v. Muschwitz, and W. Ranke, Surf. Sci. **82**, 270 (1979).
[19] K. Jacobi, Surf. Sci. **132**, 1 (1983).
[20] A. D. Katnani and D. J. Chadi, Phys. Rev. B **31**, 2554 (1985).

[21] L. Kipp, C. Janowitz, G. Mante, H. P. Barnscheidt, J. Olde, R. Manzke, and M. Skibowski, Vacuum **41**, 608 (1990).
[22] Y. Q. Cai, J. D. Riley, R. C. G. Leckey, J. Faul, and L. Ley, Phys. Rev. B **48**, 18 079 (1993).
[23] Y. Q. Cai, R. C. G. Leckey, J. D. Riley, R. Denecke, J. Faul, and L. Ley, Electron Spectrosc. Relat. Phenom. **61**, 275 (1993).
[24] M. Alonso, F. Soria, and J. L. Sacedon, J. Vac. Sci. Technol. A **3**, 1598 (1985).
[25] U. O. Karlsson, J. N. Andersen, K. Hansen, and R. Nyholm, Nucl. Instrum. Methods Phys. Res. Sect. A **282**, 553 (1989).
[26] H. Qu, P. O. Nilsson, J. Kanski, and L. Ilver, Phys. Rev. B **39**, 5276 (1989).
[27] O. K. Andersen, Phys. Rev. B **12**, 3060 (1975).
[28] P. E. S. Persson, Ph.D. thesis, Linköping Institute of Technology, 1986.
[29] L. Hedin and B. Lundquist, J. Phys. C **4**, 2064 (1971).
[30] C. Ohler, R. Kohleick, A. Förster, and H. Lüth, Phys. Rev. B **50**, 7833 (1994).
[31] C. B. M. Andersson, U. O. Karlsson, M. C. Håkansson, L. Ilver, J. Kanski, P. O. Nilsson, and L. Ö. Olsson, in *Proceedings of the 22nd International Conference on the Physics of Semiconductors, Vancouver, 1994*, edited by D. J. Lockwood (World Scientific, Singapore, 1995), p. 489.
[32] M. Taniguchi, S. Suga, M. Seki, S. Shin, K. L. I. Kobayashi, and H. Kanzaki, J. Phys. C **16**, L45 (1983).
[33] F. J. Himpsel, Appl. Opt. **19**, 3964 (1980).
[34] R. D. Bringans, R. I. G. Uhrberg, R. Z. Bachrach, and J. E. Northrup, Phys. Rev. Lett. **55**, 533 (1985).